nature portfolio

https://doi.org/10.1038/s41566-021-00943-3

Supplementary information

Observation-dependent suppression and enhancement of two-photon coincidences by tailored losses

In the format provided by the authors and unedited

Supplementary Materials for

Observation-dependent suppression and enhancement of two-photon coincidences by tailored losses

Max Ehrhardt, Matthias Heinrich, and Alexander Szameit*

University of Rostock, Institute for Physics, Albert-Einstein-Str. 23, 18059 Rostock, Germany

*Correspondence to: alexander.szameit@uni-rostock.de

This PDF file includes:

Supplementary Text

Fig. S1

Supplementary reference [S1-S4]

1. Theoretical model and polarization-dependent coupling

We describe the dynamics of single photon in our system with the Heisenberg equation of motion for the creation operators[S1]

$$\mathrm{i}\frac{\mathrm{d}}{\mathrm{dz}}\begin{pmatrix}\hat{a}_1^\dagger\\ \vdots\\ \hat{a}_N^\dagger\end{pmatrix}=\underbrace{\begin{pmatrix}0 & C_1 & & & \\ C_1 & 0 & C_2 & & 0\\ 0 & C_2 & \ddots & \ddots & \\ & & \ddots & 0 & C_{N-1}\\ & 0 & & C_{N-1} & 0\end{pmatrix}}_{\text{Hamiltonian } H}\begin{pmatrix}\hat{a}_1^\dagger\\ \vdots\\ \hat{a}_N^\dagger\end{pmatrix}$$

where C_j is the nearest-neighbor coupling strength between the waveguides $j-1$ and j. As shown in Extended Data Fig. 1, this quantity depends both on the separation of the waveguides and on the polarization of the photons propagating within them. In our experiments, the ancillary arrays were composed of 25 waveguides each, with intra-array spacings of $20\ \mu\mathrm{m}$, corresponding to coupling strengths of $C_\mathrm{H}^\mathrm{array}=0.551\ \mathrm{cm}^{-1}$ and $C_\mathrm{V}^\mathrm{array}=0.335\ \mathrm{cm}^{-1}$ for horizontally and vertically polarized photons, respectively. These arrays were placed at a distance of $27.5\ \mu\mathrm{m}$ to both sides of the target waveguide, yielding $C_\mathrm{H}=0.154\ \mathrm{cm}^{-1}$ and $C_\mathrm{V}=0.065\ \mathrm{cm}^{-1}$.

The photon's propagation dynamics are governed by the transfer matrix $U(z)=\exp(-\mathrm{i}Hz)$, and the transmission probability (Fig. 3a) of photons launched in the target waveguide ($j=13$) consequently reads $|U_{13,13}(z)|^2$. In turn, the decay rates at a position z along the direction of propagation can be calculated as $\tilde{\gamma}_{\mathrm{H/V}}(z)=-\ln\big(U_{13,13}(z)\big)/z$. Note that Zeno/Anti-Zeno dynamics render these quantities inherently z-dependent[S2,S3]. For ease of handling, we therefore introduce effective (constant) loss rates $\gamma_{\mathrm{H/V}}$ that yield the same overall attenuation after the sample length of $L=150\mathrm{mm}$, as illustrated in Fig. 3 of the main manuscript. These quantities are obtained by the remaining relative intensity $I_{\mathrm{H/V}}$ in the target waveguide (shown in Fig. 3b) via $\gamma_{\mathrm{H/V}}=-\ln(\sqrt{I_{\mathrm{H/V}}})/L$. For a relative intensities $I_{\mathrm{H(V)}}=4.5\%\ (48.3\%)$ they take the values of $\gamma_{\mathrm{H(V)}}=0.1035\ \mathrm{cm}^{-1}\ (0.02433\ \mathrm{cm}^{-1})$.

2. **Two-photon correlations and HOM visibility in the lossy polarization coupler**

In the following, we compare the two-photon correlation [S4] $\Gamma^{\mathrm{ind}}_{\mathrm{B1,B2}} = \left|U_{\mathrm{B1,D}}U_{\mathrm{B2,A}} + U_{\mathrm{B1,A}}U_{\mathrm{B2,D}}\right|^2$ and $\Gamma^{\mathrm{dis}}_{\mathrm{B1,B2}} = \left|U_{\mathrm{B1,D}}U_{\mathrm{B2,A}}\right|^2 + \left|U_{\mathrm{B1,A}}U_{\mathrm{B2,D}}\right|^2$ as the probability for observing two-photon coincidences of (in)distinguishable photon pairs between the two orthogonal polarization basis elements $\mathrm{B1}$ and $\mathrm{B2}$, where $U_{k,j}$ denotes the amplitude when launching photons in the polarization j and observing them in the polarization k. Oriented at an angle θ with respect to the HV frame, the bosonic creation operators in the basis $\mathrm{B1/B2}$ reads as

$$\begin{pmatrix}\hat{a}^\dagger_{\mathrm{B1}}\\ \hat{a}^\dagger_{\mathrm{B2}}\end{pmatrix} = \begin{pmatrix}\cos\theta & \sin\theta\\ -\sin\theta & \cos\theta\end{pmatrix}\begin{pmatrix}\hat{a}^\dagger_{\mathrm{H}}\\ \hat{a}^\dagger_{\mathrm{V}}\end{pmatrix},$$

which for the and A/D basis simplifies to

$$\begin{pmatrix}\hat{a}^\dagger_{\mathrm{D}}\\ \hat{a}^\dagger_{\mathrm{A}}\end{pmatrix} = \frac{1}{\sqrt{2}}\begin{pmatrix}1 & 1\\ -1 & 1\end{pmatrix}\begin{pmatrix}\hat{a}^\dagger_{\mathrm{H}}\\ \hat{a}^\dagger_{\mathrm{V}}\end{pmatrix}.$$

As described in the main manuscript, photons propagating in the H (fast) and V (slow) principal axes of the birefringent target waveguide accumulate the respective phase factors $e^{-\mathrm{i}\beta_{\mathrm{H}}z} = e^{-\mathrm{i}(\bar{\beta}-\Delta\beta)z}$ and $e^{-\mathrm{i}\beta_{\mathrm{V}}z} = e^{-\mathrm{i}(\bar{\beta}+\Delta\beta)z}$. Also taking into account the transmission amplitudes $e^{-\gamma_{\mathrm{H}}z} = e^{-(\bar{\gamma}+\Delta\gamma)z}$ and $e^{-\gamma_{\mathrm{V}}z} = e^{-(\bar{\gamma}-\Delta\gamma)z}$ determined by the differential losses between H and V, the photons are transferred with

$$\begin{pmatrix}\hat{a}^\dagger_{\mathrm{B1}}\\ \hat{a}^\dagger_{\mathrm{B2}}\end{pmatrix} = \begin{pmatrix}\cos\theta & \sin\theta\\ -\sin\theta & \cos\theta\end{pmatrix}\begin{pmatrix}e^{-\mathrm{i}(\bar{\beta}-\Delta\beta)z}e^{-(\bar{\gamma}+\Delta\gamma)z} & 0\\ 0 & e^{-\mathrm{i}(\bar{\beta}+\Delta\beta)z}e^{-(\bar{\gamma}-\Delta\gamma)z}\end{pmatrix}\begin{pmatrix}\hat{a}^\dagger_{\mathrm{H}}\\ \hat{a}^\dagger_{\mathrm{V}}\end{pmatrix}.$$

For the initial condition of launching a pair of photons in the A/D basis, i.e. one polarized diagonally and the other antidiagonally, one finds the following expression for the creation operators in the B1/B2 basis after a distance z:

$$\begin{pmatrix}\hat{a}^\dagger_{\mathrm{B1}}(z)\\ \hat{a}^\dagger_{\mathrm{B2}}(z)\end{pmatrix} = \frac{e^{-\mathrm{i}\bar{\beta}z}e^{-\bar{\gamma}z}}{\sqrt{2}}\begin{pmatrix}e^{\mathrm{i}(\Delta\beta+\mathrm{i}\Delta\gamma)z}\cos\theta + e^{-\mathrm{i}(\Delta\beta+\mathrm{i}\Delta\gamma)z}\sin\theta & e^{-\mathrm{i}(\Delta\beta+\mathrm{i}\Delta\gamma)z}\sin\theta - e^{\mathrm{i}(\Delta\beta+\mathrm{i}\Delta\gamma)z}\cos\theta\\ e^{-\mathrm{i}(\Delta\beta+\mathrm{i}\Delta\gamma)z}\cos\theta - e^{\mathrm{i}(\Delta\beta+\mathrm{i}\Delta\gamma)z}\sin\theta & e^{\mathrm{i}(\Delta\beta+\mathrm{i}\Delta\gamma)z}\sin\theta + e^{-\mathrm{i}(\Delta\beta+\mathrm{i}\Delta\gamma)z}\cos\theta\end{pmatrix}\begin{pmatrix}\hat{a}^\dagger_{\mathrm{D}}(0)\\ \hat{a}^\dagger_{\mathrm{A}}(0)\end{pmatrix}.$$

Accordingly, the correlation functions for indistinguishable and distinguishable photon pairs read as

$$\Gamma^{\mathrm{ind}}_{\mathrm{B1,B2}} = e^{-4\bar{\gamma}z}\left|\cos(2z(\Delta\beta + \mathrm{i}\Delta\gamma))\right|^2\ \sin^2 2\theta$$

and

$$\Gamma_{\mathrm{B1,B2}}^{\mathrm{dis}} = \frac{e^{-4\bar{\gamma}z}}{4}\left(|\cos(2z(\Delta\beta + \mathrm{i}\Delta\gamma)) \cdot \sin 2\theta + 1|^2 + |\cos(2z(\Delta\beta + \mathrm{i}\Delta\gamma)) \cdot \sin 2\theta - 1|^2\right),$$

respectively. The visibility $v = \Gamma_{\mathrm{B1,B2}}^{\mathrm{ind}}/\Gamma_{\mathrm{B1,B2}}^{\mathrm{dis}} - 1$ of HOM traces recorded under these conditions can therefore be calculated as

$$v = \frac{|\cos 2(\Delta\beta + \mathrm{i}\Delta\gamma)z|^2 \ \sin^2 2\theta}{|\cos(2z(\Delta\beta + \mathrm{i}\Delta\gamma)) \cdot \sin 2\theta + 1|^2/4 \ + |\cos(2z(\Delta\beta + \mathrm{i}\Delta\gamma)) \cdot \sin 2\theta - 1|^2/4} - 1.$$

Figure 4c of the main manuscript depicts the theoretical values of v for the waveguide system used in our experiments, whereas Supplementary Fig. S1 gives an overview of the loss dependence. Notably, in the strongly non-Hermitian limit ($\gamma \to \infty$), one finds that v becomes entirely independent of the propagation phase $\Delta\beta \cdot z$ and assumes a value of $v = +1$ in any observation basis that is not perfectly aligned with the HV frame, i.e.

$$v \xrightarrow{\gamma \to \infty} \begin{cases} -1 \text{ for } \theta = 0 \\ +1 \text{ for } \theta \neq 0 \end{cases}.$$

Experimentally, an approximation of this extremal case can be observed by substituting the photonic chip with a standard polarizing beam splitter cube that selectively blocks the transmission in one of the elements of the B1/B2 basis. Extended Data Fig. 2 shows the HOM traces recorded in such a setting. For any orientation angle θ at which photon correlations could be recorded, a distinct HOM peak with near unity visibility was observed. As the overall correlation count rate is modulated with the sine of 2θ, it vanishes in the HV basis ($\theta = 0°$ where the conventional HOM dip ($v = -1$) would otherwise remain.

3. Observation-independent fermionic quantum interference in the lossless limit ($\boldsymbol{\Delta\gamma = 0}$)

In the following we analyze the two-photon coincidences in the polarization coupler (discussed in Section 2) for fermionic two-particle exchange phase of π, yielding the two photon correlation function of $\Gamma_{\mathrm{B1,B2}}^{\mathrm{ferm}} = \left|U_{\mathrm{B1,D}}U_{\mathrm{B2,A}} - U_{\mathrm{B1,A}}U_{\mathrm{B2,D}}\right|^2 = e^{-4\bar{\gamma}z}$ and a HOM visibility

$$v^{\mathrm{ferm}} = \frac{\Gamma_{\mathrm{B1,B2}}^{\mathrm{ferm}}}{\Gamma_{\mathrm{B1,B2}}^{\mathrm{dis}}} - 1 = \frac{4}{|\cos(2z(\Delta\beta + \mathrm{i}\Delta\gamma)) \cdot \sin 2\theta + 1|^2 \ + |\cos(2z(\Delta\beta + \mathrm{i}\Delta\gamma)) \cdot \sin 2\theta - 1|^2} - 1.$$

In the Hermitian limit ($\Delta\gamma = 0$) a balanced splitting ratio ($\Delta\beta z = \pi/4$) in the polarization coupler leads to a basis(θ)-independent visibility $v = 1$.

Supplementary Figures

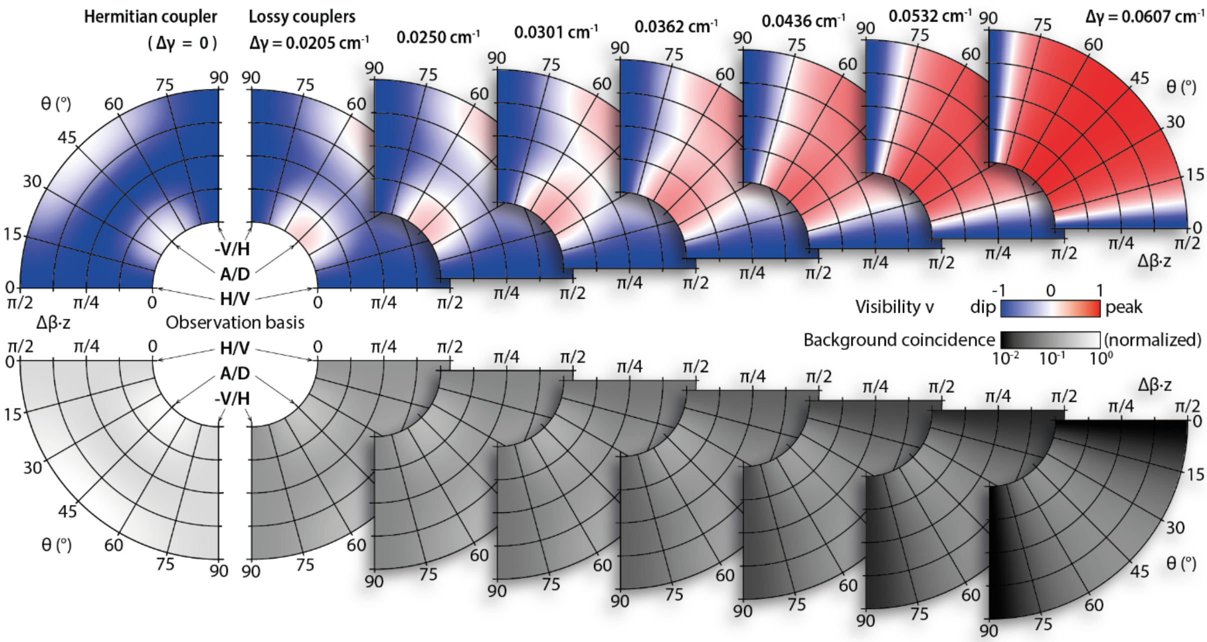

Figure S1. Impact of the overall losses on the HOM dynamics in non-Hermitian couplers. Shown are the calculated theoretical basis-dependent visibilities (top row) and background coincidence counts (bottom row) for loss contrasts $\Delta\gamma$ between 0.0205cm^{-1} and 0.0607cm^{-1} compared to the Hermitian case ($\Delta\gamma = 0$). Note that, as $\Delta\gamma$ increases, the peak visibility approaches 1 and becomes independent of the coupling phase $\Delta\beta \cdot z$. Simultaneously, the transition between HOM dip and peak becomes sharper. As a result, towards the strongly non-Hermitian limit, dips can only be observed in those bases that are ever more closely aligned with the HV frame, and, as such, are also subject to the strongest overall damping of the background coincidence rate.

Supplementary References

S1 Lai, W. K., Buek, V. & Knight, P. L. Nonclassical fields in a linear directional coupler. *Phys. Rev. A* **43**, 6323–6336 (1991).

S2 Longhi, S. Optical Bloch oscillations and Zener tunneling with nonclassical light. *Phys. Rev. Lett.* **101**, 193902 (2008).

S3 Dreisow, F., Szameit, A., Heinrich, M., Pertsch, T., Nolte, S., Tünnermann, A. & Longhi, S. Decay Control via Discrete-to-Continuum Coupling Modulation in an Optical Waveguide System. (2008).

S4 Bromberg, Y., Lahini, Y., Morandotti, R. & Silberberg, Y. Quantum and Classical Correlations in Waveguide Lattices. *Phys. Rev. Lett.* **102**, 253904 (2009).